

(Cyclopentadienyl)iron(II) Complexes of N-Heterocyclic Carbenes Bearing a Malonate or Imidate Backbone: Synthesis, Structure, and Catalytic Potential in Hydrosilylation

Vincent César,^{*,†,‡} Luis C. Misal Castro,[§] Thomas Dombay,[§] Jean-Baptiste Sortais,^{*,§} Christophe Darcel,[§] Stéphane Labat,^{||} Karinne Miqueu,^{||} Jean-Marc Sotiropoulos,^{||} Rémy Brousses,^{†,‡} Noël Lugan,^{*,†,‡} and Guy Lavigne^{†,‡}

[†]CNRS, LCC (Laboratoire de Chimie de Coordination), 205 route de Narbonne, 31077 Toulouse Cedex 4, France

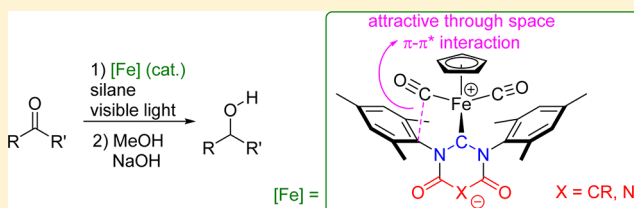
[‡]Université de Toulouse, UPS, INPT, 31077 Toulouse, France

[§]UMR 6226 CNRS-Université de Rennes 1, "Institut des Sciences Chimiques de Rennes", Centre for Catalysis and Green Chemistry-Team "Organometallics: Materials and Catalysis", Campus de Beaulieu, 35042 Rennes Cedex, France

^{||}Institut des Sciences Analytiques et de Physico-Chimie pour l'Environnement et les Matériaux (UMR 5254), Equipe Chimie Physique, Université de Pau et des Pays de l'Adour, Hélioparc, 2 Avenue du Président Angot, 64053 Pau Cedex 09, France

Supporting Information

ABSTRACT: The backbone-functionalized anionic carbenes *malo*NHC (**1_R**; malonate backbone) and *imid*NHC (**2**; imidate backbone) were generated in situ from their respective zwitterionic precursors and treated with FeCp(CO)₂I to afford the zwitterionic complexes {FeCp(CO)₂(**1_R**)} (**3_R**; 59–84% yield), and {FeCp(CO)₂(**2**)} (**4**; 77% yield), respectively. Methylation of the malonate complex **3_{Me}** takes place at one of the backbone oxygen atoms to give the cationic adduct [FeCp(CO)₂(**1_{Me}^{Me}**)](OTf) ([**5^{Me}**](OTf); 96% yield), whereas methylation of **4** takes place at the imidate nitrogen atom to produce the cationic adduct [FeCp(CO)₂(**2^{Me}**)](OTf) ([**6^{Me}**](OTf); 84% yield). All of the complexes were characterized by NMR and IR in solution, while X-ray structure analyses were carried out for **3_{Me}**, **4**, and [**6^{Me}**](OTf). In addition, a detailed experimental and theoretical investigation of the electron density within the archetypal zwitterionic complex **3_{Me}** was carried out. The observation of short intramolecular contacts between C_{ipso} or C_{ortho} of the mesityl groups of the carbene and the proximal carbonyl groups is rationalized in terms of a noncovalent "through space" π–π* interaction involving a two-electron delocalization of the occupied π(C_{ipso}=C_{ortho}) molecular orbital (MO) of the aryl ring into one vacant π*(C≡O) MO of the carbonyl ligand. A theoretical analysis carried out on dissymmetrical model complexes reveals that the magnitude of such an interaction is correlated with the donor properties of aryl group substituents. A catalyst screening of the above complexes in the hydrosilylation of benzaldehyde under visible light irradiation revealed a dramatic effect of the electronic donor properties of these carbenes on the performances of their complexes, with the more nucleophilic carbene **1_{tBu}** in the zwitterionic species **3_{tBu}** appearing as the most efficient. This complex shows good efficiency and excellent chemoselectivity in the hydrosilylation of various aldehydes bearing reactive functional groups. It is also moderately active in the hydrosilylation of a few ketone substrates and exhibits very good performance in the hydrosilylation of representative aldimines and ketimines.



INTRODUCTION

Whereas major contemporary advances in organometallic catalysis rest on the utilization of noble metal complexes, the perspective of developing sustainable alternatives based on first-row transition metals is now appearing as an important challenge of the new millennium. Iron is particularly valuable in such a view as a cheap, abundant, and environmentally benign element. As a consequence, intense research on the catalytic potential of its complexes has emerged during the past decade.^{1,2}

Polydentate ligands have been extensively used for the elaboration of *well-defined* iron-based precatalysts, just because the presence of several donor atoms is prone to counterbalance

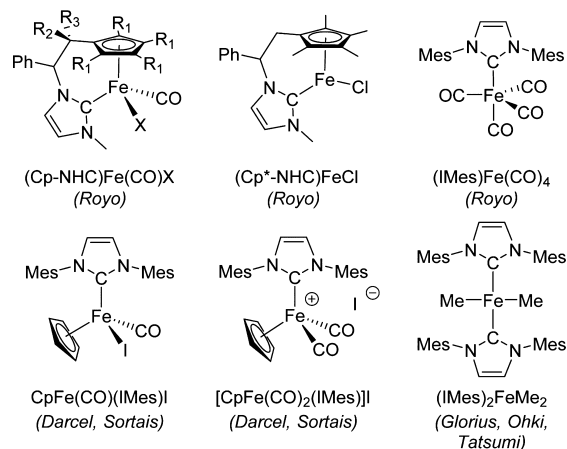
the inherent weakness of Fe–element bonds.³ To this end, N-heterocyclic carbenes (NHC)^{4,5} are also of particular interest as strong electron donors, either for the construction of chelating architectures^{6,7} or as simple *monodentate* ligands.⁸

Building on the pioneering work of Brunner on the catalytic activity of [CpFe(CO)(X)] species in hydrogenation and hydrosilylation,⁹ Royo reported in 2010 that various N-heterocyclic carbene tethered cyclopentadienyl complexes such as (Cp-NHC)Fe(CO)X (X = Cl, I) and the 16e complex (Cp*-NHC)FeCl are active catalysts in the transfer hydro-

Received: June 28, 2013

genation of ketones and the hydrosilylation of aldehydes and sulfoxides (Chart 1).^{10,11} Independently, in a parallel approach,

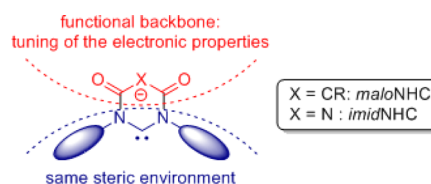
Chart 1. Literature Examples of Well-Defined NHC-Fe Complexes Used as Precatalysts in the Hydrosilylation of Carbonyl Functionalities



Darcel, Sortais, and co-workers explored in detail the catalytic potential of simple (cyclopentadienyl)iron complexes incorporating the monodentate 1,3-dimesitylimidazol-2-ylidene IMes, namely, $[\text{CpFe}(\text{CO})_2(\text{IMes})]^+\text{I}^-$ and $\text{CpFe}(\text{CO})(\text{IMes})\text{I}$, which had been previously reported by Guerchais.^{12,13} Upon activation by visible light, these complexes were found to efficiently catalyze the hydrosilylation of various unsaturated molecules such as aldehydes, ketones, amides, and imines.¹² More recently, Ohki, Tatsumi, and Glorius reported the new square-planar bis(N-heterocyclic carbene) complexes $(\text{IMes})_2\text{FeMe}_2$, which proved to be active in the transfer hydrogenation of 2'-acetonaphthone at very low catalyst loading.¹⁴ Finally, the archetype of a NHC-Fe(0) complex $(\text{IMes})\text{Fe}(\text{CO})_4$ was synthesized by Royo and shown to catalyze the hydrosilylation of benzaldehyde.^{15a} Very recently, using the same complex under very mild conditions, Sortais, Darcel, and co-workers reported the selective reduction of esters to aldehydes.^{15b}

Considering the practical advantages and broad availability of simple cyclopentadienyl-NHC piano-stool iron complexes of the type $[\text{CpFe}(\text{CO})_2(\text{NHC})]^+$, and following a recent investigation of the influence of the NHC's steric parameters on the hydrosilylation reaction,^{12c} we were prompted to study the effect of a modulation of the electronic donor properties of the N-heterocyclic carbene on the efficiency of the catalyst. Among the few existing categories of electronically switchable/tunable N-heterocyclic carbenes,¹⁶ we were logically inclined to select members of our previously reported series of backbone-functionalized N-heterocyclic carbenes,^{17–19} in particular, those incorporating a malonate¹⁷ or imidate¹⁸ unit as the remote component of their heterocyclic framework (Chart 2). Indeed, their expected advantages are the following: (1) these anionic carbenes can readily displace halides from various transition-metal complexes to afford zwitterionic derivatives (the first archetype of a zwitterionic Fe complex incorporating a malonic NHC was briefly disclosed as part of our original preliminary communication);^{17a} (2) their electronic properties can be finely tuned after their complexation to various transition metals, without affecting the steric environment they provide around the metal center.

Chart 2. Schematic Representation of the Anionic NHCs under Investigation

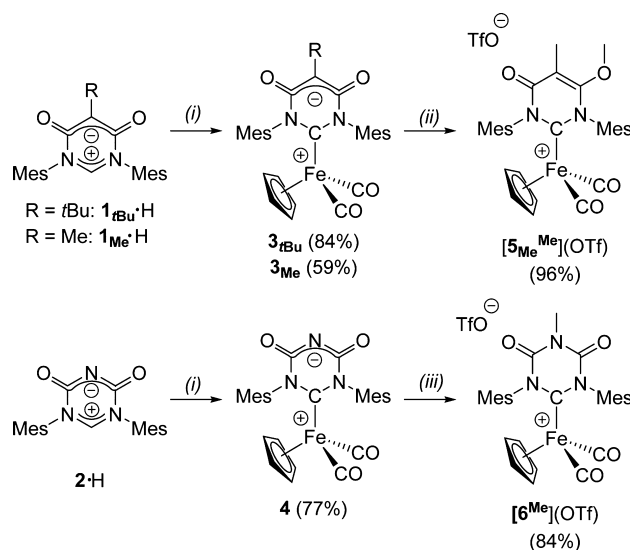


The present report deals with the preparation and characterization of five new piano-stool (cyclopentadienyl)iron complexes incorporating diversely functionalized NHCs and includes an evaluation of their scope as precatalysts in hydrosilylation. During the course of this work, the structural characterization of the complexes was strengthened by a detailed charge density analysis performed on one representative zwitterionic complex, giving an instructive view of its electronic system and offering a rationale for the recurrence of a very characteristic attractive intramolecular interligand interaction between one of the aryl substituents of the carbene and an adjacent carbonyl group.

RESULTS AND DISCUSSION

Synthesis and Spectroscopic Characterization of the NHC-Iron(II) Complexes. The potassium salt of the anionic carbene $[\mathbf{1}_R]^- \text{K}^+$ was generated in situ by deprotonation of the corresponding pyrimidinium betaine $\mathbf{1}_R\text{-H}$ with KHMDS. Its addition to the precursor $\text{CpFe}(\text{CO})_2\text{I}$ was found to take place with spontaneous displacement of the iodide, to give the desired zwitterionic complex $[\text{CpFe}(\text{CO})_2(\mathbf{1}_R)]$ ($\mathbf{3}_R$) (Scheme 1).²⁰ However, whereas the previously prepared $\mathbf{3}_{t\text{Bu}}$ could be easily purified by simple washings with Et_2O after having filtered off the KCl precipitate from a CH_2Cl_2 solution,^{17a} this procedure could not be duplicated for the preparation of $\mathbf{3}_{\text{Me}}$, since the crude product of the latter was contaminated by small amounts of the pyrimidinium precursor $\mathbf{1}_{\text{Me}}\text{-H}$. Nevertheless,

Scheme 1. Synthesis of the Zwitterionic and Cationic Complexes 3–6^a



^aConditions: (i) (1) KHMDS, THF, 0 °C, 15 min, (2) $\text{CpFe}(\text{CO})_2\text{I}$, 25 °C, overnight; (ii) MeOTf, CH_2Cl_2 , 0 °C, 2 h; (iii) MeOTf, CH_2Cl_2 , -40 °C, 2 h. Isolated yields are indicated.

efficient purification could be achieved by flash chromatography under an inert atmosphere. Under these optimized conditions, 3_{tBu} was obtained in good yield (84%), while the yield for 3_{Me} was found to be slightly lower (59%). The imidate-derived zwitterionic complex $[\text{CpFe}(\text{CO})_2(\mathbf{2})]$ ($\mathbf{4}$) was obtained from the corresponding mesoionic precursor $\mathbf{2}\cdot\text{H}$, following a parallel procedure. In that case, complex $\mathbf{4}$, which is totally insoluble in THF, was seen to precipitate during the course of the reaction and could thus be easily isolated in pure form by filtration and further extraction from a CH_2Cl_2 solution (to remove the inorganic KCl salt). Further independent treatment of the zwitterionic complexes 3_{Me} and $\mathbf{4}$ with methyl triflate led to the corresponding cationic complexes $[\mathbf{5}_{\text{Me}}^{\text{Me}}](\text{OTf})$ and $[\mathbf{6}^{\text{Me}}](\text{OTf})$, respectively. Methylation of the malonate complex takes place at one of the exocyclic oxygen atoms, whereas methylation of the imidate backbone takes place at the central nitrogen atom.

All five complexes were fully characterized in solution by spectroscopic methods and for four of them, namely 3_{Me} , 3_{tBu} ,^{17a} $\mathbf{4}$, and $[\mathbf{6}^{\text{Me}}](\text{OTf})$, by an X-ray structure analysis. A rough estimate of the respective ligand-donating abilities of the five carbenes can be obtained from the average value of the ν_{CO} stretching frequencies of the two IR stretching bands of the carbonyl ligands (Table 1). Such $\nu_{\text{CO}}^{\text{av}}$ values are roughly

Table 1. Summary of Meaningful Spectroscopic Data

entry	complex	NHC	$\delta(\text{N}_2\text{C})$ (ppm)	$\nu_{\text{CO}}^{\text{av}}$ (cm^{-1}) ^a	TEP value (cm^{-1}) ^b
1	3_{tBu}	$\mathbf{1}_{\text{tBu}}^-$	193.2	2016	2042
2	3_{Me}	$\mathbf{1}_{\text{Me}}^-$	194.9	2017	2042.5
3	$[\mathbf{5}_{\text{Me}}^{\text{Me}}](\text{OTf})$	$\mathbf{1}_{\text{Me}}^{\text{Me}}$	212.6	2027	2051
4	$\mathbf{4}$	$\mathbf{2}^-$	214.1	2023	2049
5	$[\mathbf{6}^{\text{Me}}](\text{OTf})$	$\mathbf{2}^{\text{Me}}$	230.7	2031	2058 ^c

^a $\nu_{\text{CO}}^{\text{av}}$ is the average value of the frequencies of the two CO stretching bands (recorded in solution in CH_2Cl_2). ^bThe TEP values were calculated from the corresponding $\text{LRh}(\text{CO})_2\text{Cl}$ using the linear regressions developed by Plenio and Nolan.²¹ ^cSince $(\mathbf{2}^{\text{Me}})\text{Rh}(\text{CO})_2\text{Cl}$ is unknown, the TEP value was taken from $(\mathbf{2}^{\text{H}})\text{Rh}(\text{CO})_2\text{Cl}$.

correlated with the Tolman electronic parameters (TEPs) of the corresponding carbenes, which were previously determined from the IR spectra of their corresponding standard carbonylrhodium(I) complexes *cis*-(NHC)RhCl(CO)₂ using Plenio's and Nolan's correlations.^{17c,18,21} The present carbenes can thus be ranked from the best donors to the poorest ones, in the following order: $\mathbf{1}_{\text{tBu}}^- \approx \mathbf{1}_{\text{Me}}^- > \mathbf{2}^- > \mathbf{1}_{\text{Me}}^{\text{Me}} > \mathbf{2}^{\text{Me}}$. Whereas the anionic carbenes $\mathbf{1}_{\text{R}}^-$ and $\mathbf{2}^-$ are the most electron-donating carbenes, the methylation of the backbone leads in both cases to a significant decrease of the electronic donor properties, as previously discussed in our earlier work.^{17c,18} Accordingly, the resulting alkylated derivatives now belong to new classes of NHCs: the O-methylated carbene $\mathbf{1}_{\text{Me}}^{\text{Me}}$ should be regarded as an archetype of amino-acrylamidocarbene,^{17c,22} whereas the spectral characteristics of the N-methylated carbene $\mathbf{2}^{\text{Me}}$ appear comparable with those ascribed to a six-membered diamidocarbene.^{17b,23} It is also noteworthy that the respective values of the ¹³C chemical shifts of their carbenic carbon center are also roughly negatively correlated with the electronic donor properties of the carbene (Table 1). However, this is an indication which, taken alone, is generally not regarded as a sufficiently reliable probe, since it may be subject to a rather broad variability depending on other factors.²⁴

Molecular Structures of the NHC-Iron(II) Complexes 3–6. These complexes all exhibit a three-legged piano-stool geometry comparable with that of the classical cationic complex $[\text{CpFe}\{\text{IMes}\}(\text{CO})_2]^+\text{I}^-$ previously prepared from the neutral N-heterocyclic carbene IMes (Figure 1).¹³ However, given that

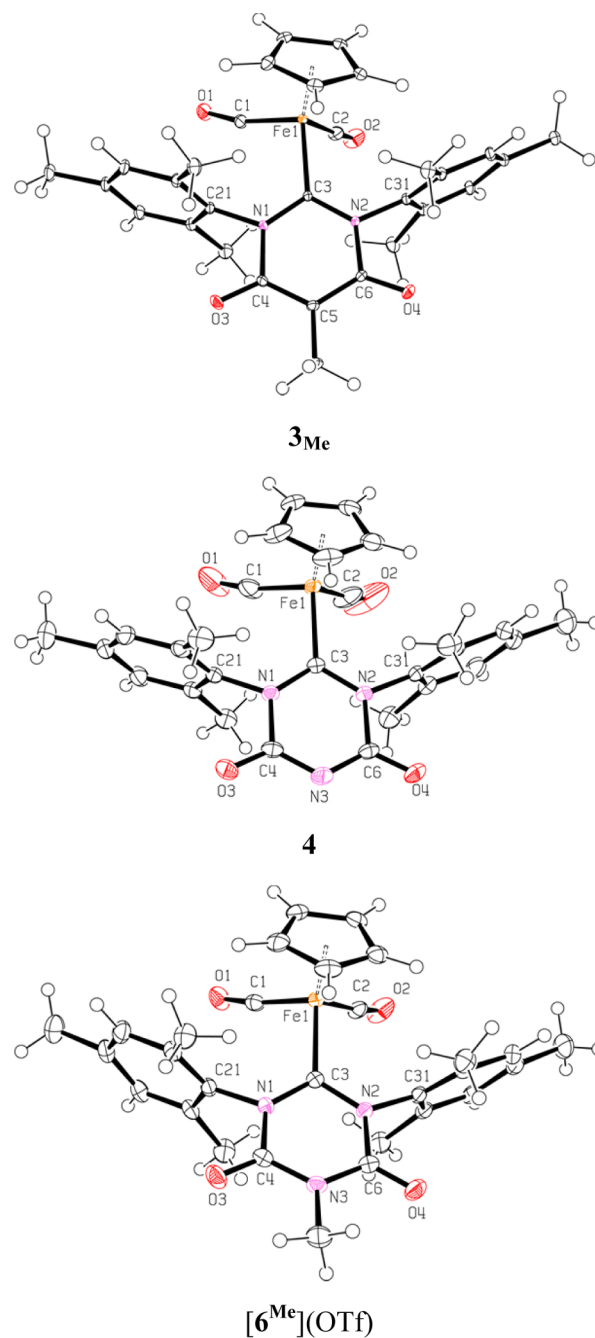
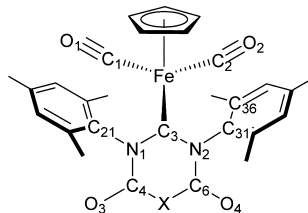


Figure 1. Molecular structures of complexes 3_{Me} , $\mathbf{4}$, and $[\mathbf{6}^{\text{Me}}](\text{OTf})$ with thermal ellipsoids drawn at the 30% probability level. The triflate anion in $[\mathbf{6}^{\text{Me}}](\text{OTf})$ has been omitted for clarity.

the orientation of the nitrogen substituents is determined by the heterocyclic ring size, the steric bulk of the present six-membered-ring carbenes is higher than that of classical five-membered NHCs and ensures a better shielding of the metal's cavity. A comparative analysis of geometrical parameters over this series of molecular complexes is quite instructive, since all the N-heterocyclic carbenes encountered here exhibit roughly

Table 2. Selected Bond Distances and Angles for Complexes 3_{tBu} , 3_{Me} , **4**, and $[6^{Me}](OTf)^a$ 

bond or angle ^b	3_{tBu}	$n_{Pauling}^c$	3_{Me}	$n_{Pauling}^c$	n_{topo}^c	4	$n_{Pauling}^c$	$[6^{Me}](OTf)$	$n_{Pauling}^c$
Fe–C3	2.041(1)		2.0439(2)			2.031(2)		2.003(2)	
C3–N1	1.351(2)	1.3	1.3553(3)	1.3	1.2	1.353(2)	1.3	1.362(2)	1.2
C3–N2	1.353(2)	1.3	1.3623(3)	1.3	1.3	1.356(2)	1.3	1.370(2)	1.3
N1–C4	1.462(2)	0.9	1.4550(3)	0.9	1.1	1.464(2)	0.9	1.423(2)	1.0
N2–C6	1.473(2)	0.9	1.4625(3)	0.9	1.0	1.464(2)	0.9	1.423(2)	1.0
C4–O3	1.237(2)		1.2409(4)			1.221(2)		1.198(2)	
C6–O4	1.237(2)		1.2358(4)			1.219(2)		1.205(2)	
C4–X	1.403(2)	1.5	1.3961(3)	1.5	1.6	1.330(2)	1.9	1.374(2)	1.7
C6–X	1.405(2)	1.5	1.4010(3)	1.5	1.5	1.333(2)	1.9	1.365(2)	1.7
C1...C21	2.884(2)		2.7197(4)			2.867(2)		2.856(2)	
C2...C36	2.969(2)		3.0518(5)			3.001(2)		2.930(2)	
Fe–C1–O1	169.9(1)		165.5(4)			168.7(2)		171.3(2)	
Fe–C2–O2	170.1(1)		174.0(1)			171.8(2)		172.0(2)	

^aFor comparative purposes, the values reported for the previously reported complex 3_{tBu} are also included.^{17a} ^bInteratomic distances in Å and bond angles in deg. ^cParameters taken from ref 27 (the model 2 was chosen for the calculation of n_{topo}).

the same steric bulk and differ only in the magnitude of their respective electronic donor properties. Table 2 shows a compilation of selected interatomic distances and bond angles for the above complexes, from which the following conclusions can be drawn: the observed geometries of the anionic N-heterocyclic carbenes within the zwitterionic complexes 3_{Me} and 3_{tBu} are consistent with our view^{17a} of their framework as a juxtaposition between two independent electronic π systems, namely, the proximal diaminocarbene unit NCN (a delocalized four- π -electron system), on which a distal malonate unit (a delocalized six- π -electron system) is grafted, with only little or no electronic communication between the two π systems. Effectively, the values of the C–C and C=O bond distances over the anionic malonate moiety are intermediate between standard single and double bonds, thus corresponding to a delocalized structure featuring two mesomeric forms with alternate double and single bonds. In addition, the bonds N1–C4 and N2–C6 connecting this anionic backbone unit to the proximal carbenic moiety exhibit an average value of 1.463 Å, clearly falling into the range of prototypical single $C_{sp^2}-N_{sp^2}$ bonds (1.45–1.47 Å).²⁵ Similar observations can be made about the geometry of the heterocycle of **2** in **4**, where the magnitude of bond lengths reflects an electronic delocalization over the remote anionic imidate unit O=C–N[–]–C=O, whereas, again, the single-bond character of the two C–N bonds connecting it to the neutral carbenic moiety is indicative of the absence of electronic communication between the proximal and distal parts of the heterocycle. Interestingly, the situation changes upon alkylation of the remote nitrogen of **2**, producing the cationic complex $[6^{Me}](OTf)$. Clearly, the alkylation is accompanied by a lengthening of the two equivalent backbone C–N bonds that are connecting the imidate nitrogen N3 to the lateral carbonyls. Typically, C4–N3 evolves from 1.333(2) to 1.372(2) Å, whereas C6–N3 evolves from 1.330(2) to 1.365(2) Å. Simultaneously, we see a shortening of both $C_{sp^2}-N_{sp^2}$ type bonds N1–C4 and N2–

C6 from 1.464(2) to 1.423(2) Å. A rationale for these experimental observations is that the nitrogen p^π lone pairs on N1 and N2, which were originally engaged in the stabilization of the carbenic center C3 in complex **4**, are becoming much less available for that purpose in $[6^{Me}](OTf)$, due to their electronic delocalization over the lateral amide moieties. A bond order evaluation according to Pauling's model^{26,27} nicely reflects these variations (Table 2). Such a change in the electronic structure of the carbene **2**^{Me} is also reflected by the observation that the metal–carbene bond length Fe–C3 = 2.0032(15) Å in $[6^{Me}](OTf)$ is significantly reduced with respect to its original value of 2.0305(14) Å in **4**. Such a shrinking can be reasonably rationalized in terms of the occurrence of π back-bonding in $[6^{Me}](OTf)$ from the metal center into the more accessible vacant $2p^\pi$ of the carbene center of **2**^{Me}²⁸ and is consistent with its formulation as a diamidocarbene.

Striking geometrical features readily observable in the solid-state structures of complexes 3_{tBu} , 3_{Me} , **4**, and $[6_{Me}]^+$ are (i) the pronounced bent structure of the carbonyl ligands and (ii) the proximity between the carbon atoms of these carbonyls and both the *ipso* and *ortho* carbon atoms of the mesityl groups of the N-heterocyclic carbene, respectively, leading to the relatively short interligand distances C1–C21 and C2–C36 (Table 2). A closer view of the structure reveals that the molecule does not perfectly adopt the schematic idealized mirror plane symmetry represented in Table 2. Indeed, due to the possibility of free rotation around the Fe–C3 bond, one can observe a dissymmetrization where one of these distances, C1...C21, becomes significantly shorter than the other distance, C2...C36. Closely related structural peculiarities—i.e. the presence of bent CO ligands in the vicinity of an aryl ring—were previously stressed in a series of Fischer-type manganese aryloxycarbene complexes of the type $Cp(CO)_2Mn=C(Ph)-OAr$ ²⁹ and were originally rationalized by some of us in terms of a noncovalent “through space” $\pi-\pi^*$ interaction involving a two-electron delocalization of the occupied $\pi(C_{ipso}=C_{ortho})$

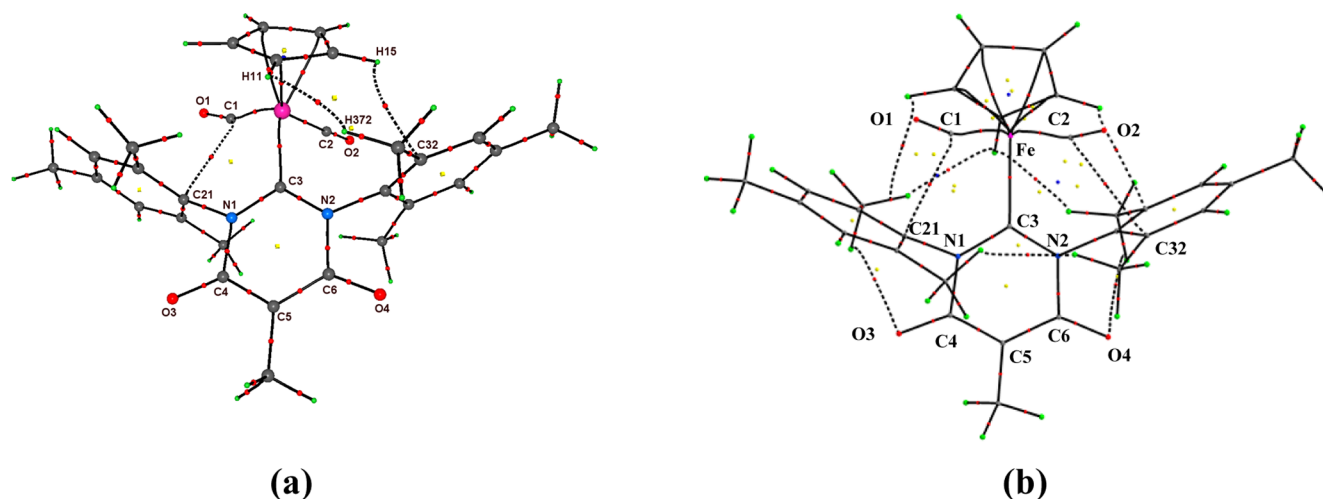


Figure 2. Experimental (a) and theoretical (b) molecular graphs for complex 3_{Me} (black lines are bp's, red dots are bcp's, yellow dots are rcp's, and small blue dots are ccp's; non-CP threshold arbitrarily set to 0.008 au in the theoretical molecular graph).

Table 3. AIM and NBO Analyses of the Weak Interligand Interactions in Complex 3_{Me} at the M06-2X/6-31G** Level of Theory

AIM Analysis of the C(aryl)⋯C(≡O) Bond Critical Points contact		R_b^a	$\rho(r_b)^b$	$\nabla^2\rho(r_b)^c$	$G\rho(r_b)^d$	$V\rho(r_b)^d$	$\delta(C\cdots C)^e$	E_{int}^f
C1⋯C21	exptl ^g	2.7197(4)	0.13	1.15	0.08	-0.08	n/a	3.9
	calcd ^h	2.811	0.11	1.16	0.07	-0.06	0.05	3.1
C2⋯C36 ⁱ	exptl	3.0518(5)						
	calcd	2.908	0.08	0.95	0.05	-0.04	0.02	2.0
NBO analysis								
$\pi_{\text{C}=\text{C}} \rightarrow \pi_{\text{C}=\text{O}}$ interaction involved in the major $\text{C}_{\text{Mes}}\cdots\text{C}_{\text{CO}}$ contact			$\pi_{\text{C}=\text{C}} \rightarrow \pi_{\text{C}=\text{O}}$ interaction involved in the minor $\text{C}_{\text{Mes}}\cdots\text{C}_{\text{CO}}$ contact					
$\Delta E(2)^j$ $\pi_{\text{C}=\text{C}} \rightarrow \pi_{\text{C}=\text{O}}$	NLMO ^k $\pi_{\text{C}=\text{C}}$				$\Delta E(2)^j$ $\pi_{\text{C}=\text{C}} \rightarrow \pi_{\text{C}=\text{O}}$	NLMO ^k $\pi_{\text{C}=\text{C}}$		
4.4	C ₂₁ , 43.8% C ₂₆ , 38.8% C ₁ , 0.6% O ₁ , 0.2%	3.4			C ₃₁ , 43.5% C ₃₆ , 39.1% C ₂ , 0.3% O ₂ , 0.1%			

^a R_b is the interatomic distance (Å). ^b $\rho(r_b)$ is the ED ($\text{e } \text{Å}^{-3}$). ^c $\nabla^2\rho(r_b)$ is the Laplacian of the ED ($\text{e } \text{Å}^{-5}$). ^d $G\rho(r_b)$ and $V\rho(r_b)$ are the kinetic and potential electron energy densities, respectively, estimated using the approximation of Abramov⁴² (hartree Å^{-3}). ^e $\delta(C\cdots C)$ are the delocalization indices.⁴³ ^f E_{int} is the interaction energy estimated using the Espinoza correlation scheme (kcal mol^{-1}).^{40,41} ^gexptl = experimental value. ^hcalcd = theoretical value from isolated molecule DFT calculations. ⁱFor the weak interactions C(aryl)⋯C(≡O) either the C_{ipso} (labeled C₃₁) or C_{ortho} (labeled C₃₆) carbon atom of the aryl group is involved. ^jStabilizing energy in kcal mol^{-1} . ^kNatural Localized Molecular Orbital associated with the $\pi_{\text{C}=\text{C}}^{\text{aryl}}$ orbital involved in the weak interaction $\pi_{\text{C}=\text{C}}^{\text{aryl}} \rightarrow \pi_{\text{C}=\text{O}}$.

molecular orbital (MO) of the aryl ring into one vacant $\pi^*(\text{C}\equiv\text{O})$ MO of the carbonyl ligand. Experimental evidence for the occurrence of such noncovalent intermolecular interactions was previously obtained by examining the topology of the electron density within one representative example: namely, $\text{Cp}(\text{CO})_2\text{Mn}=\text{C}(\text{Ph})(\text{O}(2,4,6\text{-Cl}_3\text{Ph}))$ in the framework of Bader's QTAIM. In the same previous work, it was also suggested that similar noncovalent interactions are actually present in a variety of NHC/carbonyl complexes and, very importantly, in NHC/carbene complexes, including Grubbs

type II complexes, with possible consequences on their catalytic activity.^{29b,30}

Taking advantage of the availability of high-quality single crystals of 3_{Me} , we seized the opportunity to effectively examine for the first time the topology of the experimental electron density within an N-aryl-substituted NHC/iron carbonyl complex.³¹

Detailed Experimental and Theoretical Investigation of the Electron Density, within the Archetypal Zwitterionic Complex 3_{Me} . The experimental electron density (ED)

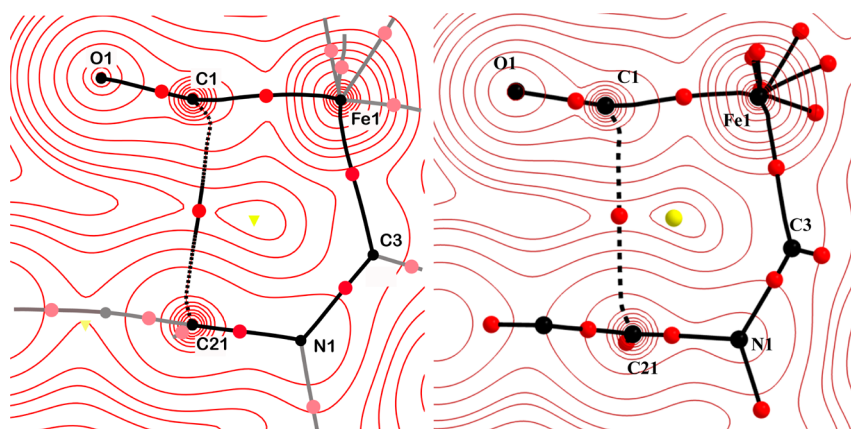


Figure 3. Experimental (left) and theoretical (right) isocontours of $\rho(r_b)$ in the Fe1/C1/C21 plane (red lines), including bcp's (red dots), rcp's (yellow dots), and bp's (black lines) within or close to that plane.

distribution $\rho(r_b)$ within 3_{Me} was established from a high-resolution XRD data set using the multipole formalism of Hansen and Coppens.³² For the sake of comparison, the theoretical ED distribution was also established from DFT calculations on the basis of the gas-phase optimized geometry of the complex.³³ Gratifyingly, the initial screening of different DFT functionals (Table S4, Supporting Information) revealed that M06-2X, which integrates dispersion terms, is well suited for reproducing the experimentally observed asymmetry of the complex noted above and characterized by slight differences between intramolecular interligand bonds such as C1...C21 and C2...C31 that might be a priori expected to be formally equivalent (Table S5, Supporting Information). Deviations of these computed C...C distances from the experimental values do not exceed 2% (2.811 versus 2.720 Å and 3.105 versus 3.183 Å). The other geometrical parameters involving the carbene ligand and the metallic fragment also satisfactorily reproduce experimental values, particularly the Fe–C_{carbene} bond length (2.072 versus 2.044 Å) and the Fe–C–O bond angle (165.49 versus 165.45° and 169.77 versus 173.95°) with only a deviation of 1.2% relative to the experimental data. Hence, the electronic structure and the topological analysis of complex 3_{Me} were investigated at the M06-2X/6-31G** level of theory. It appears that the match between experimental and theoretical values is generally good (Table S6, Supporting Information), except for the C–O bonds, as is often the case.³⁴ The experimental (a) and theoretical (b) molecular graphs are depicted in Figure 2 and confirm the satisfactory match between the two approaches.³⁵

All bond critical points (bcp's) corresponding to anticipated bonds within the *malo*NHC 1_{Me}^- , CO, and Cp ligands are observed. The topological parameters at these points, corresponding to high values of the electron density $\rho(r_b)$, negative values of the Laplacian $\nabla^2\rho(r_b)$, and negative values of the total energy density $H(r_b)$, reflect the existence of associated shared-shell (covalent) interactions, as expected. The bond orders within the NHC ring, now calculated by taking into account the values of electron density and the Laplacian following the model of Howard et al.,²⁷ show the same trend as those derived from Pauling's model, although the differences in bond orders are less pronounced (Table 2). A total of six bcp's are detected around the Fe center in the experimental molecular graph. Two are associated with the Fe–CO bonds, one with the Fe–carbene bond, and three only with the Fe–Cp linkage, where five are expected³⁶ and are actually

observed in the theoretical molecular graph. Topological parameters at these bcp's, which show relatively low values of $\rho(r_b)$, small positive values of $\nabla^2\rho(r_b)$, and small negative values of $H(r_b)$ with $G(r_b)/\rho(r_b) \approx 1$, are typical of ligand–metal bonds³⁷ and compare well with those found experimentally in relevant low-valent transition-metal complexes, including a chromium NHC complex³¹ and other iron organometallic complexes.³⁸

As a matter of fact, the experimental molecular graph also shows three extra intramolecular interligand bcp's. The first one, clearly exhibiting the highest $\rho(r_b)$ value of 0.13 e Å⁻³ (Table 3), is located approximately at mid distance between the *ipso* carbon C21 of the Mes group attached to N1 and the carbon atom C1 of the proximal CO ligand (a cross-section view of this interaction is provided in Figure 3). The topological parameters at this bcp are characterized by a low value of $\rho(r_b)$ and a positive value for $\nabla^2\rho(r_b)$, indicative of the occurrence of a weak closed-shell interaction between these atoms,³⁹ thus providing the first experimental evidence for a C_{*ipso*}(aryl)...C–[M] interaction within an N-heterocyclic carbene complex of a first-row transition element. The corresponding interaction energy E_{int} was estimated to be 3.9 kcal mol⁻¹ using the Espinosa correlation scheme.^{40,41} This value is significantly higher than that originally detected in the previously investigated Mn(I) aryloxycarbene (2.8 kcal mol⁻¹).²⁹ The interaction energies corresponding to the other two contacts, C32...H15 and H11...H37, which also necessarily participate in the stabilization of the complex, were estimated to be 2.5 and 1.7 kcal mol⁻¹, respectively.

Gratifyingly, the computed molecular graph corresponding to the optimized gas-phase geometry reveals the occurrence of the aforementioned matching weak interligand interaction C1–C21, associated with a value of 3.1 kcal mol⁻¹ for E_{int} (Table 3, Figure 3), thereby indicating that such an interaction cannot be the result of packing effects. The graph also reveals the occurrence of a C2...C36 interaction similar in nature to the C1...C21 interaction (Figure 2), albeit weaker in terms of interaction energy (2.0 kcal mol⁻¹), which is not detected experimentally (Table 3). The bcp's located between the *ipso* carbon C21 of the Mes group the carbon atom C1 of the CO moiety exhibits a density value $\rho(r_b)$ of 0.11 e Å⁻³ (Table 3), in agreement with the experimental data. Moreover, a smaller value of 0.08 e Å⁻³ is calculated for the other intramolecular interaction between C36 and C2. In addition, the theoretical molecular graph also reveals additional weak H...O interactions

between the hydrogen atoms of the mesityl group and the oxygen atoms of the malonate moiety. Beyond the existence of bcp's between C1 and C21 in both the experimental and theoretical ED distribution, additional computational evidence for the occurrence of a weak noncovalent interaction between these atoms was inferred from the weak, albeit significant, value of 0.05 for the $\delta(C1,C21)$ delocalization index^{4,5} and from the second-order perturbation (SOP) theory of the NBO method, which revealed a stabilizing two-electron delocalization from the $\pi(C_{ipso}=C_{ortho})$ to the $\pi^*(C\equiv O)$ molecular orbitals with a $\Delta E(2)$ value of 4.4 kcal mol⁻¹ for the associated SOP energy (Table 3), similar in essence to that originally evidenced in the aforementioned Mn(I) aryloxycarbene complex.²⁹ Moreover, the Natural Localized Molecular Orbital (NLMO) associated with the $\pi_{C21=C26}^{Mes}$ orbital of the aryl ring directed toward the C₁≡O ligand presents a weak participation of the $\pi^*_{C1\equiv O}$ orbital (% C, 0.6; and % O, 0.2), in agreement with the existence of a weak noncovalent interaction between C1 and C21 (Table 3). It is worth noting that the NLMO corresponding to the $\pi_{C31=C36}^{Mes}$ orbital of the other aryl ring also reveals a weak participation of the $\pi^*_{C2\equiv O}$ orbital (% C, 0.3; % O, 0.1), the latter being less important than the previous and corresponding to a $\pi_{C31=C36}^{Mes} \rightarrow \pi^*_{C2\equiv O}$ stabilizing energy $\Delta E(2)$ of 3.4 kcal mol⁻¹ (Table 3).

To gain more insight into the characteristics of these weak interligand interactions, further calculations on the electronic structure and topological analysis were carried out on complexes **4** and [6^{Me}](OTf) as well as on model dissymmetrical complexes **7** and **8** with electronically discriminated N-aryl substituents and/or a N-methyl substituent (see the Supporting Information, Tables S12 and S13). Clearly, whereas the magnitude of the interaction appeared to be unaffected by the electronic donicity of the carbene center, it was found to be more sensitive to the electron richness of the aryl ring, being strengthened by the adjunction of a donor *p*-NMe₂ substituent and diminished by an electron-withdrawing *p*-NO₂ group on the aryl ring. This extends the number of reported examples of organometallic complexes where attractive vs repulsive intramolecular interligand interactions are taking place between a $\pi_{C=C}$ orbital belonging to an aryl group and $\pi^*_{C\equiv O}$ of an adjacent carbonyl ligand.

Evaluation of the Complexes as Hydrosilylation Catalysts. The first optimization of the experimental conditions of the hydrosilylation reaction was carried out with benzaldehyde **9** as the model substrate and complex **3_{tBu}** as the precatalyst. The relevant results are summarized in Table 4. In a first test reaction, the optimized reaction conditions (Table 4, entries 1 and 2) which had been previously determined for the cationic complex [CpFe(CO)₂(IMes)]⁺I⁻ (**11**) were applied to this system and, to our delight, a full conversion was obtained after 3 h, leading to benzyl alcohol **10** as the single product, after a classical base-promoted hydrolysis of the silylated ether intermediate. Given that, just like **11**, complex **3_{tBu}** is a saturated 18e⁻ complex, its *in situ* activation upon irradiation by visible light appears necessary and constitutes a simple and convenient means to create coordinative insaturation by loss of CO (Table 4, entry 3). An examination of the influence of the nature of the silane revealed that diphenylsilane, methylphenylsilane, or the activated trisubstituted silanes Me(EtO)₂SiH and (EtO)₃SiH lead to full conversions after 1 or 3 h, whereas triethylsilane and tetramethyldisiloxane (TMDS) are not suitable as hydride sources in this catalysis. Furthermore, although it has been

Table 4. Optimization for the Reduction of Benzaldehyde with Catalyst **3_{tBu}^a**

entry	silane	cat. loading (mol %)	time (h)	conv (%) ^b
1	PhSiH ₃	1	1	89
2	PhSiH ₃	1	3	98
3 ^c	PhSiH ₃	1	3	0
4	PhSiH ₃	0.5	1	72
5	Ph ₂ SiH ₂	1	1	97
6	Ph ₂ SiH ₂	1	3	98
7	Ph ₂ SiH ₂	0.5	1	97
8	MePhSiH ₂	1	1	85
9	MePhSiH ₂	1	3	98
10	Et ₃ SiH	1	3	0
11	Me(EtO) ₂ SiH	1	1	83
12	Me(EtO) ₂ SiH	1	3	92
13	(EtO) ₃ SiH	1	1	94
14	TMDS ^d	1	3	0

^aTypical procedure: benzaldehyde (0.5 mmol), silane (0.5 mmol), and complex **3_{tBu}** (0.5–1 mol %) were stirred at 30 °C in THF (1 mL) under visible light irradiation; the reaction mixture was then hydrolyzed at room temperature for 2 h with methanol (2 mL) and 2 M aqueous NaOH (2 mL). ^bConversion determined by GC after methanolysis. ^cWithout visible light irradiation. ^dTMDS = tetramethyldisiloxane.

previously observed in some cases that steric hindrance may have a deleterious effect on the activity,^{12c} the catalytic efficiency of complex **3_{tBu}** bearing a bulky carbene appears to be higher than that of **11**, leading in particular to full conversion within only 1 h with diphenylsilane as a reactant (Table 4, entry 5). A further advantage is its preserved efficiency at low catalyst loading (Table 4, entry 7), possibly reflecting a higher stability.⁴⁴ The only drawback is that **3_{tBu}** is much sensitive toward traces of acid, which tend to reduce its activity, possibly by adventitious protonation of its backbone, as previously observed with other transition metals.^{17c} Here, this is simply avoided by using freshly distilled benzaldehyde.

Following the above optimization, we were prompted to determine the influence of the electronic properties of the carbene on the performances of the catalyst. The comparative evaluation of the electronically tuned NHC ligands, using diphenylsilane as the selected hydride source, is displayed in Table 5. The zwitterionic complexes **3_{Me}** and **3_{tBu}**, incorporating the more nucleophilic carbenes, clearly appear as the best catalysts (Table 5, entries 2 and 3). The fact that their respective performances are equivalent indicates that the nature of the apical substituent on the malonate backbone has no effect on the catalysis. This means that, in contrast with what was previously observed in the Rh-catalyzed hydroboration of styrene,^{17c} the substrate does not interfere with the backbone oxygen atoms. In addition, the three other iron complexes are inactive under these conditions at 30 °C (Table 5, entries 4, 6, and 8), though their activity is restored upon increasing the reaction temperature up to 70 °C. At that temperature, a full conversion was observed after 3 h using [5^{Me}](OTf) (entry 5), whereas the diamidocarbene–iron complex [6^{Me}](OTf)

Table 5. Hydrosilylation of Benzaldehyde using Complexes $3_{\text{R}}-[6^{\text{Me}}](\text{OTf})^{\text{a}}$

entry	Fe complex	T ($^{\circ}\text{C}$)	conv (%) ^b
1	3_{tBu}	30	97
2	3_{Me}	30	98
3 ^c	3_{Me}	30	93
4	$[5_{\text{Me}}^{\text{Me}}](\text{OTf})$	30	<5
5	$[5_{\text{Me}}^{\text{Me}}](\text{OTf})$	70	98
6	4	30	<5
7	4	70	18
8	$[6^{\text{Me}}](\text{OTf})$	30	<5
9	$[6^{\text{Me}}](\text{OTf})$	70	40

^aTypical conditions: benzaldehyde (0.5 mmol), silane (0.5 mmol), and Fe complex (1 mol %) were stirred at the indicated temperature in THF (1 mL) under visible light irradiation for 3 h; the reaction mixture was then hydrolyzed with methanol (2 mL) and 2 M aqueous NaOH (2 mL). ^bConversion determined by GC after hydrolysis. ^cCatalyst loading 0.5 mol %.

displayed a poor activity with 40% conversion after 3 h (Table 5, entry 9). These differences in activity can be correlated with the electronic properties of the supporting NHC ligands, with the more electron-donating anionic carbenes 1_{R}^{-} giving the more active precatalysts 3_{R} . By the way, it should be noted that the lack of activity of the zwitterionic complex **4** (Table 5, entries 6 and 7), apparently inconsistent with the good nucleophilicity of its carbene, is in fact due only to its total insolubility in THF.

In further work, the optimized experimental conditions defined above were used to examine the scope of the iron precatalyst 3_{tBu} in the hydrosilylation of a variety of aldehydes, ketones, and imines. The results are presented in Table 6. When the reaction was carried out with benzaldehydes bearing electronically different *para* substituents (Table 6, entries 1–4), a full conversion was obtained, suggesting that the electronic effects on the reactivity are limited, even if more favorable hydrosilylation conditions (PhSiH₃ in neat conditions) had to be used for some substrates (Table 6, entries 2 and 3). The chemoselectivity is also excellent, since a nitrile group or a triple C–C bond were tolerated as aryl *para* substituents of the aldehyde under such conditions (Table 6, entries 3 and 4). An *ortho* substitution is also not deleterious for the issue of the reaction with 2-methylbenzaldehyde being reduced in good yield (Table 6, entry 5), but the catalytic system was found to be inefficient for reducing cinnamyl aldehyde, an archetype of α -enal.

The optimized conditions (1 mol % of catalyst 3_{tBu} , 1.2 equiv of Ph₂SiH₂ in THF under visible light irradiation) were also employed for the reduction of some representative ketones. As in previous reports,^{12a} the temperature and reaction time had to be increased to respectively 70 $^{\circ}\text{C}$ and 16 h to observe a noticeable catalytic activity. Under these conditions, moderate to good yields were obtained for the tested ketones (Table 6, entries 7, 9 and 11). Better yields were obtained when the reactions were carried out with the more reactive phenylsilane under neat conditions (Table 6, entries 8 and 10), as previously noted.^{12c} Nevertheless, complex 3_{tBu} appeared to be not as efficient as its parent cationic complex **11** for the ketone substrates. One possible explanation could be that the steric hindrance brought about the iron center by the ligand 1_{tBu}^{-} is too high and tends to limit the approach of the bulkier ketones. Finally, for a complete comparative survey of the catalytic

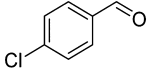
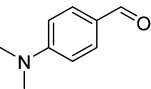
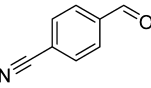
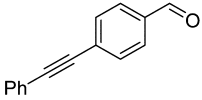
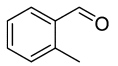
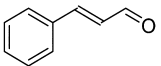
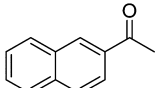
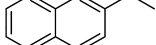
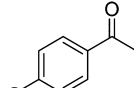
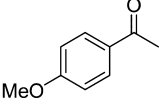
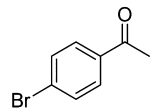
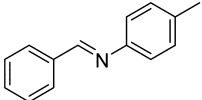
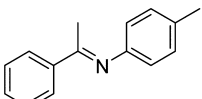
potential of this system, we turned our attention to the hydrosilylation of two prototypes of aldimines and ketimines, whose reduction was efficiently achieved with complex **11** (5 mol % catalyst, PhSiH₃ (4 equiv), neat, 30 $^{\circ}\text{C}$, 30 h for the aldimine and 100 $^{\circ}\text{C}$, 24 h for the ketimine).^{12d} In this reaction, complex 3_{tBu} proved to be a suitable precatalyst, affording the corresponding amines in excellent yield in the case of the ketimine (Table 6, entry 12) and in an average yield starting from the aldimine (Table 6, entry 13).

CONCLUSION

The goal of the present work was to examine the catalytic scope and possible limitations of anionic six-membered-ring N-heterocyclic carbene ligands incorporating a malonate or an imidate backbone, as substitutes for classical neutral N-heterocyclic carbene ligands within a series of (cyclopentadienyl)iron carbonyl complexes known to be active in hydrosilylation. These anionic ligands, *malo*NHC (1_{R}^{-}) and *imid*NHC (2^{-}), are prone to displace the iodide from FeCp(CO)₂I to afford the zwitterionic complexes {FeCp(CO)₂(1_{R})} (3_{R}) and {FeCp(CO)₂(2)} (**4**), which were fully characterized. A modulation of the donor properties of the carbene in such complexes was readily achieved by addition of methyl triflate, which interacts selectively either with one oxygen of the malonate backbone or with the nitrogen of the imidate backbone to give the cationic adducts [FeCp(CO)₂(1_{R}^{Me})](OTf) ($[5^{\text{Me}}](\text{OTf})$) and [FeCp(CO)₂(2^{Me})](OTf) ($[6^{\text{Me}}](\text{OTf})$), respectively. Importantly, all carbenes investigated here exhibit the same steric bulk and present variable nucleophilicities, following the order $1_{\text{R}}^{-} > 2^{-} > 1_{\text{Me}}^{\text{Me}} > 2^{\text{Me}}$. A catalyst screening of the above complexes in the hydrosilylation of benzaldehyde under visible irradiation revealed a dramatic effect of the electronic donor properties of the carbenes on the performances of their complexes, with the more nucleophilic carbene 1_{tBu}^{-} in the zwitterionic species 3_{tBu} appearing as the more efficient. This complex shows good efficiency and excellent chemoselectivity in the hydrosilylation of various aldehydes bearing reactive functional groups. It is also moderately active in the hydrosilylation of a few ketone substrates and exhibits good performances in the hydrosilylation of representative aldimine and ketimine.

In parallel to the above work, a thorough examination of the electron density distribution (ED) within the representative complex 3_{Me} was carried out on the basis of a high-resolution X-ray analysis, complemented by a DFT analysis at the M06-2X/6-31G** level of theory, which includes dispersion terms. Gratifyingly, the experimental structure was reproduced in its finest details, and a perfect match between experimental and theoretical ED maps was obtained. In particular, the observation of a short intramolecular contact between C_{ipso} (or C_{ortho}) of one of the mesityl groups of the carbene and the closest of the two carbonyl groups was rationalized in terms of a noncovalent “through space” π – π^* interaction involving a two-electron delocalization of the occupied π (C_{ipso}=C_{ortho}) molecular orbital (MO) of the aryl ring into one vacant π^* (C≡O) MO of the carbonyl ligand. A theoretical analysis carried out on dissymmetrical model complexes, and presented as Supporting Information, reveals that the magnitude of such an attractive interaction is correlated with the donor properties of aryl group substituents.

Table 6. Scope of the Iron-Catalyzed Hydrosilylation of Unsaturated Compounds using Complex 3_{tBu} ^a

Entry	substrate	silane (equiv.)	solvent	T(°C)/t(h)	conv. (yield) ^b
1		Ph ₂ SiH ₂ (1.0)	THF	30/1	>98 (83)
2		PhSiH ₃ (1.2)	neat	30/3	>98 (82)
3		PhSiH ₃ (1.2)	neat	30/3	96 (95)
4		Ph ₂ SiH ₂ (1.0)	THF	30/3	97 (96)
5		Ph ₂ SiH ₂ (1.0)	THF	30/1	98 (72)
6		Ph ₂ SiH ₂ (1.0)	THF	30/3	0
7		Ph ₂ SiH ₂ (1.2)	THF	70/16	72 (70)
8		PhSiH ₃ (1.2)	neat	70/16	>98 (94)
9		Ph ₂ SiH ₂ (1.2)	THF	70/16	37 (30)
10		PhSiH ₃ (1.2)	neat	70/16	50 (50)
11		Ph ₂ SiH ₂ (1.2)	THF	70/16	58 (47)
12 ^c		PhSiH ₃ (4.0)	neat	30/30	88 (53)
13 ^c		PhSiH ₃ (4.0)	neat	100/24	>98 (93)

^aTypical conditions: substrate (1 mmol), silane (1–4 equiv), and precatalyst 3_{tBu} (1 mol %) were stirred in THF or neat at the indicated temperature upon visible light irradiation for the indicated time; the reaction mixture was then hydrolyzed with methanol (2 mL) and 2 M aqueous NaOH (2 mL) at room temperature for 2 h. ^bConversion determined by ¹H NMR after methanolysis; in parentheses, isolated yields after purification by column chromatography are given in parentheses. ^c5 mol % of 3_{tBu} was used.

EXPERIMENTAL SECTION

Materials and Methods. All manipulations were performed under an inert atmosphere of dry nitrogen by using standard vacuum line and Schlenk tube techniques. Glassware was dried at 120 °C in an oven for at least 3 h. THF and diethyl ether were distilled from sodium/benzophenone and toluene from sodium. Pentane, dichloromethane, and chloroform were dried over CaH₂ and subsequently distilled. NMR spectra were recorded on Bruker ARX250, AV30, and AV400 spectrometers. Chemical shifts are reported in ppm (δ) in comparison to TMS (¹H and ¹³C) using the residual peak of deuterated solvent as an internal standard.⁴⁵ Infrared spectra were obtained on a Perkin-Elmer Spectrum 100 FT-IR spectrometer. MS spectra were performed by the mass spectrometry service of the "Institut de Chimie de Toulouse". CpFe(CO)₂I,⁴⁶ pyrimidinium betaines $1_{Me}\cdot H$ and $1_{tBu}\cdot H$,¹⁷

and triazin-1-ium-3-ide $2\cdot H$ ¹⁸ were synthesized following literature procedures.

(η^5 -Cyclopentadienyl)dicarbonyl(1,3-dimesityl-5-*tert*-butyl-6-oxo-6*H*-pyrimidin-2-ylidene-4-olate)iron(II) (3_{tBu}). A solution of KHMDS (0.5 M in toluene, 5.4 mL, 2.69 mmol, 1.1 equiv) was added dropwise to a solution of $1_{tBu}\cdot H$ (990 mg, 2.45 mmol) in THF (35 mL) at room temperature. After 15 min, CpFe(CO)₂I (743 mg, 2.45 mmol, 1.0 equiv) was added as a solid. The mixture turned bronze and was stirred for 3 h. Volatiles were evaporated, and the residue was purified by flash chromatography under an N₂ atmosphere (SiO₂, CH₂Cl₂/MeOH 95/5). The yellow-brown band was collected to give, after evaporation and drying, the title complex as an ochre powder (1.2 g, 84%). X-ray-quality crystals were grown by layering a solution of 3_{tBu} in CH₂Cl₂ with Et₂O. Spectroscopic and analytical characterizations have been previously reported.^{17a}

(η^5 -Cyclopentadienyl)dicarbonyl(1,3-dimesityl-5-methyl-6-oxo-6H-pyrimidin-2-ylidene-4-olate)iron(II) (3_{Me}). A solution of KHMDS (0.5 M in toluene, 4.6 mL, 2.30 mmol, 1.1 equiv) was added dropwise to a solution of $1_{Me}\cdot H$ (762 mg, 2.10 mmol) in THF (35 mL) at room temperature. After 30 min, the solution was cooled to $-40^\circ C$ and $CpFe(CO)_2I$ (638 mg, 2.10 mmol, 1.0 equiv) was added as a solid. After 1 h, the cooling bath was removed and the solution was stirred overnight at room temperature. Volatiles were evaporated, and the crude residue was purified by flash chromatography under N_2 (SiO_2 , $CH_2Cl_2/MeOH$ 95/5). The dark yellow band was collected and was evaporated. A further washing with Et_2O (2×5 mL) gave the pure complex as an orange powder (670 mg, 59%). X-ray-quality crystals were grown by layering a solution of 3_{Me} in CH_2Cl_2 with Et_2O . Mp: 192–194 $^\circ C$ dec. 1H NMR (400 MHz, $CDCl_3$): δ 6.96 (s, 4H, CH_{Mes}), 4.74 (s, 5H, CH_{Cp}), 2.35 (s, 6H, CH_3_{para}), 2.15 (s, 12H, CH_3_{ortho}), 1.94 (s, 3H, CH_3_{apical}). ^{13}C NMR (100.5 MHz, $CDCl_3$): δ 209.0 (Fe-CO), 195.0 (N_2C), 162.1 (C-O), 142.8, 138.7, 136.8 (C_{Mes}), 129.5 (CH_{Mes}), 90.1 (C_{apical}), 86.7 (CH_{Cp}), 21.2 (CH_3_{para}), 19.0 (CH_3_{ortho}), 9.1 (CH_3_{apical}). IR (ATR): $\tilde{\nu}$ 3099, 3039, 2920, 2858, 2025, 1989, 1980, 1622, 1481, 1430, 1384, 1346, 1292, 1224, 1166, 1055, 1020, 861, 854, 842, 835, 779, 760 cm^{-1} . IR (CH_2Cl_2): ν_{CO} 2039, 1995 cm^{-1} . MS (ESI): m/z (%) 539 (100) [$M + H$] $^+$. HR-MS (ESI): m/z calcd for $C_{30}H_{31}N_2O_4^{54}Fe$ 537.1680, found 537.1639.

(η^5 -Cyclopentadienyl)dicarbonyl(1,3-dimesityl-4,6-dioxo-1,3,5-triazinan-5-ide-2-ylidene)iron(II) (**4**). A solution of KHMDS (0.5 M in toluene, 3.85 mL, 1.92 mmol, 1.1 equiv) was added dropwise to a solution of **2** $\cdot H$ (612 mg, 1.75 mmol) in THF (25 mL) at $0^\circ C$. After 20 min, $CpFe(CO)_2I$ (531 mg, 1.75 mmol, 1.0 equiv) was added as a solid, the cooling bath was removed, and the solution was stirred overnight. A yellow precipitate appeared along the reaction course. The supernatant dark solution was filtered away, and the solid residue was washed with Et_2O (2×10 mL). After drying, it was taken up with CH_2Cl_2 (10 mL) and filtered through Celite (10 mL more to rinse) to give an orange-yellow powder (700 mg, 77%). X-ray-quality crystals were grown by layering a solution of **4** in CH_2Cl_2 with Et_2O . Mp: 176 $^\circ C$ dec. 1H NMR (400 MHz, CD_2Cl_2): δ = 7.02 (s, 4H, CH_{Mes}), 4.77 (s, 5H, CH_{Cp}), 2.77 (s, 6H, CH_3_{para}), 2.16 (s, 12H, CH_3_{ortho}). ^{13}C NMR (100.5 MHz, CD_2Cl_2): δ 214.5 (N_2C), 209.0 (Fe-CO), 152.5 (C-O), 141.9, 139.9, 136.9 (C_{Mes}), 129.7 (CH_{Mes}), 87.2 (CH_{Cp}), 21.1 (CH_3_{para}), 19.1 (CH_3_{ortho}). IR (ATR): $\tilde{\nu}$ 3092, 2954, 2921, 2860, 2024, 2036, 1992, 1982, 1718, 1641, 1441, 1431, 1374, 1297, 1273, 1233, 1068, 1022, 1010, 875, 844, 780, 768 cm^{-1} . IR (CH_2Cl_2): ν_{CO} 2045, 2002 cm^{-1} . MS (ESI): m/z (%) 526 (100) [$M + H$] $^+$. HR-MS (ESI): m/z calcd for $C_{28}H_{28}N_3O_4^{54}Fe$ 524.1476, found 524.1437.

(η^5 -Cyclopentadienyl)dicarbonyl(1,3-dimesityl-4-oxo-4H-5-methyl-6-methoxy-pyrimidin-2-ylidene)iron(II) Trifluoromethanesulfonate ([5_{Me}^{Me}](OTf)). Methyl triflate (50 μL , 0.457 mmol, 1.0 equiv) was added dropwise to a solution of 3_{Me} (246 mg, 0.457 mmol) in CH_2Cl_2 (10 mL) at $0^\circ C$. After addition, the cooling bath was removed and the solution was stirred for 2 h. After filtration through Celite (to remove some paramagnetic decomposition), the solution was concentrated to about 0.5 mL and the product was precipitated by addition of Et_2O . The supernatant solution was removed via cannula, and the solid was dried to give the product as a yellow powder (310 mg, 96%). Mp: 146–147 $^\circ C$ dec. 1H NMR (400 MHz, CD_2Cl_2): δ 7.14 (s, 2H, CH_{Mes}), 7.11 (s, 2H, CH_{Mes}), 4.90 (s, 5H, CH_{Cp}), 3.69 (s, 3H, OCH_3), 2.42 (s, 3H, CH_3_{para}), 2.41 (s, 3H, CH_3_{para}), 2.16 (s, 6H, CH_3_{ortho}), 2.11 (s, 3H, CH_3_{apical}), 2.08 (s, 6H, CH_3_{ortho}). ^{13}C NMR (100.5 MHz, CD_2Cl_2): δ 213.0 (N_2C), 208.0 (Fe-CO), 161.4 (C-O), 160.1 (C-O), 142.1, 141.3, 140.7, 139.8, 136.4, 136.2 (C_{Mes}), 130.9, 130.6 (CH_{Mes}), 107.1 (C_{apical}), 87.7 (CH_{Cp}), 63.5 (OCH_3), 21.3 (CH_3_{para}), 19.2 (CH_3_{ortho}), 18.9 (CH_3_{ortho}), 10.0 (CH_3_{apical}). IR (ATR): $\tilde{\nu}$ 3087, 2961, 2923, 2864, 2044, 2003, 1685, 1645, 1400, 1256, 1222, 1143, 1030, 994, 849, 770 cm^{-1} . IR (CH_2Cl_2): ν_{CO} 2048, 2007 cm^{-1} . MS (ESI): m/z (%) 553 (47) [$M - OTf$] $^+$, 377 (100) [$M - OTf - CpFe(CO)_2$] $^+$. HR-MS (ESI): m/z calcd for $C_{31}H_{33}N_2O_4^{54}Fe$ 553.1784, found 553.1805.

(η^5 -Cyclopentadienyl)dicarbonyl(1,3-dimesityl-5-methyl-4,6-dioxo-1,3,5-triazinan-2-ylidene)iron(II) Trifluoromethane-

sulfonate ([6^{Me}](OTf)). Methyl triflate (33 μL , 0.295 mmol, 1.0 equiv) was added dropwise to a solution of **4** (155 mg, 0.295 mmol) in CH_2Cl_2 (10 mL) at $-40^\circ C$, and the solution was stirred at that temperature for 2 h. After it was warmed to room temperature, the reaction mixture was filtered through Celite to remove a dark brown precipitate formed during the reaction. The crude solution was then concentrated to about 1 mL, and addition of Et_2O led to the precipitation of a bright yellow precipitate. The solution was filtered away, and the solid was dried to yield the product as a canary yellow powder (170 mg, 84%). Single crystals suitable for an X-ray diffraction experiment were grown by layering Et_2O onto a solution of [6^{Me}](OTf) in CH_2Cl_2 . Mp: 180 $^\circ C$ dec. 1H NMR (400 MHz, CD_2Cl_2): δ 7.11 (s, 4H, CH_{Mes}), 5.07 (s, 5H, CH_{Cp}), 3.46 (s, 3H, NCH_3), 2.40 (s, 6H, CH_3_{para}), 2.24 (s, 12H, CH_3_{ortho}). ^{13}C NMR (100.5 MHz, CD_2Cl_2): δ 230.6 (N_2C), 206.9 (Fe-CO), 144.9, 141.5, 139.3, 136.6 ($C_{Mes} + C=O$), 130.4 (CH_{Mes}), 87.5 (CH_{Cp}), 30.5 (NCH_3), 20.8 (CH_3_{para}), 18.8 (CH_3_{ortho}). IR (ATR): $\tilde{\nu}$ 3093, 2047, 2011, 1765, 1712, 1606, 1428, 1414, 1377, 1281, 1264, 1250, 1226, 1152, 1036, 1022, 1002, 856, 847, 766 cm^{-1} . IR (CH_2Cl_2): ν_{CO} 2051, 2011 cm^{-1} . MS (ESI): m/z (%) 540 (100) [$M - OTf$] $^+$, 364 (68) [($Me-imidNHC-Mes$)H] $^+$. HR-MS (ESI): m/z calcd for $C_{29}H_{30}N_3O_4^{54}Fe$ 540.1580, found 540.1596.

General Procedure A for the Iron-Catalyzed Hydrosilylation of Aldehydes. A flame-dried Schlenk flask was charged with the iron complex 3_{IBu} (5.8 mg, 10 μmol , 1 mol %) which was dissolved in anhydrous THF (1 mL). The aldehyde (1 mmol) and diphenylsilane (186 μL , 1 mmol) were added consecutively. The reaction mixture was stirred in a $30^\circ C$ preheated oil bath under light irradiation for 1 h. The reaction mixture was then hydrolyzed at room temperature for 2 h with methanol (2 mL) and a 2 M aqueous solution of sodium hydroxide (2 mL). The product was extracted with diethyl ether (3×10 mL). The combined organic layers were washed with brine, dried with sodium sulfate, and evaporated. The crude residue was purified by silica gel chromatography using a petroleum ether/diethyl ether mixture as the eluent.

General Procedure B for the Iron-Catalyzed Hydrosilylation of Ketones. A flame-dried Schlenk flask was charged with the iron complex 3_{IBu} (5.8 mg, 10 μmol , 1 mol %) which was dissolved in anhydrous THF (1 mL). The ketone (1 mmol) and diphenylsilane (223 μL , 1.2 mmol) were added consecutively. The reaction mixture was stirred in a $70^\circ C$ preheated oil bath under light irradiation for 16 h. The reaction mixture was then quenched at room temperature for 2 h with methanol (2 mL) and a 2 M aqueous solution of sodium hydroxide (2 mL). The product was extracted with diethyl ether (3×10 mL). The combined organic layers were washed with brine, dried with sodium sulfate, and evaporated. The crude residue was purified by silica gel chromatography using a petroleum ether/diethyl ether mixture as the eluent.

Normal-Resolution X-ray Diffraction Study. Data for complexes 3_{IBu} , **4**, and $6^{Me}OTf$ were mounted on a Bruker D8 APEX II diffractometer equipped with an Oxford Cryosystem N_2 gas stream low-temperature device. Data were collected at a temperature of $T = 180(\pm 1)$ K. The frames were reduced using the APEX2 suite of programs.⁴⁷ Semiempirical absorption corrections using spherical harmonics were applied using the DIFABS procedure as implemented in APEX2. The structures were solved within the WINGX suite⁴⁸ using the SIR92 program,⁴⁹ which revealed in each instance the position of most of the non-hydrogen atoms. All remaining non-hydrogen atoms were located by the usual combination of full-matrix least-squares refinement and difference electron density syntheses by using the SHELX program.⁵⁰ All non-hydrogen atoms were allowed to vibrate anisotropically. All of the hydrogen atoms were set in idealized positions ($C(sp^2)-H = 0.93$ Å; U_{iso} 1.2 times greater than the U_{eq} value of the carbon atom to which the hydrogen atom is attached) and their positions were refined as "riding" atoms.

High-Resolution X-ray Diffraction Study. A parallelepiped-shaped light orange crystal of 3^{Me} of dimensions $0.46 \times 0.46 \times 0.35$ mm³ was mounted on a Bruker D8 diffractometer equipped with an APEX II detector and an Oxford Cryosystem N_2 gas stream low-temperature device. Data were collected at a temperature of $T =$

100(\pm 1) K. The frames were reduced and corrected from absorption as above, using the APEX2 suite of programs. The resulting 319631 reflections (\langle redundancy $\rangle = 9.5$) were merged in Laue group $\bar{1}$ with the use of the program SORTAV⁵¹ to give 33477 unique reflections up to a resolution S of 1.19 \AA^{-1} ($R_{\text{int}} = 0.0257$), providing 94% of data up to $\theta < 57.8^\circ$. The multipolar refinement was conducted on a complete data set by limiting the resolution to $S = 1.10 \text{\AA}^{-1}$. Other crystallographic and data collection details are given in Tables S1 and S2 (Supporting Information).

In a first step, the crystal structure was solved using SIR92⁴⁹ and then refined in a classical manner by full-matrix least squares on F^2 using the SHELX program.⁵⁰ Details of this initial refinement are given in Table S1. Subsequent multipole refinement was carried out within the Hansen–Coppens formalism³² using the MoPro package.⁵² The positions for the hydrogen atoms were allowed to vary in a restrained model as implemented in MoPro ($C(\text{sp}^2)\text{--H} = 1.083 \text{\AA}$; $C(\text{sp}^3)\text{--H} = 1.093 \text{\AA}$), whereas their anisotropic temperature factors were estimated by the method of Madsen⁵³ using the SHADE2 web server⁵⁴ and held fixed during the multipolar refinement procedure. An electroneutrality constraint was systematically applied. The multipole expansion was truncated at the hexadecapole level ($l_{\text{max}} = 4$) for Fe and at the octupole level ($l_{\text{max}} = 3$) for C, N, and O atoms. A H–C bond directed dipole ($l_{\text{max}} = 2$) was introduced for the hydrogen atoms. The positions and the thermal parameters for non-hydrogen atoms were first refined using high-resolution data only ($1.1 > S > 0.7 \text{\AA}^{-1}$). Then the valence electron density was fitted using low-resolution data only ($S < 0.7 \text{\AA}^{-1}$) in successive cycles on P_{ν} , κ , $P_{\text{lm}\pm}$ and κ' parameters, until convergence was reached. For Fe, the multipoles were allowed to refine assuming a $3d^6$ valence configuration, the 4s electrons being set in the core. Two sets of κ/κ' parameters for the two types of chemically different O atoms (Fe–CO and C=O), a single set of κ/κ' parameters for the N atoms, and seven sets of κ/κ' parameters for the four types of chemically different C atoms (Fe–CO, Fe=C, C=O, CMe, C_5H_5 , C_{Ar} , C_{sp^3}) were used and refined. For H atoms, three different values of κ were used (CH_3 , C_5H_5 , $C_6H_2(CH_3)_3$), while the κ' parameters were fixed to 1.2. In the final cycles of refinement, all parameters were allowed to vary (within the limits of the above constraints and restraints), with data for which $I > 3\sigma(I)$, truncated at 1.1\AA^{-1} . Final multipolar parameters for complex 3_{Me} are given in Table S2.

The Hirshfeld rigid bond test⁵⁵ is respected for all light atom–light atom bonds and for the Fe–C3 bond, all $\Delta(\text{msda})$ values being less than $1.0 \times 10^{-3} \text{\AA}^2$. The remaining Fe–C bonds, however, do not totally fulfill the Hirshfeld criterion. The $\Delta(\text{msda})$ values for Fe– $C_{\text{CP ring}}$ were actually found in the range $(1.6\text{--}3.2) \times 10^{-3} \text{\AA}^2$, while for the two Fe–CO bonds, the values were 1.5×10^{-3} and $2.2 \times 10^{-3} \text{\AA}^2$, respectively. Attempts to improve those values by introducing anharmonic thermal parameters for Fe remained inconclusive; therefore, these were not considered further.

The analysis of the topology of the electron density was carried out using either the VMOPro⁵² or WinXPro program package.⁵⁶ Topological parameters at selected bond critical points in 3_{Me} are shown in Table S3 (Supporting Information), along with those resulting from the analysis of the theoretical ED distribution. The kinetic energy densities values $G(\rho)$ given in that table were estimated using the approximation of Abramov,⁴² while the corresponding potential energy densities values $V(\rho)$ were obtained from the local virial theorem: $V(\rho) = \frac{1}{4}\nabla^2\rho(\mathbf{r}) - 2G(\rho)$.

Computational Details. Calculations were carried out with the Gaussian 09 program³³ at the DFT level of theory using the M06-2X functional.⁵⁷ All of the atoms (C, N, H, O, Fe) have been described with a 6-31G(d,p) double- ζ basis set.⁵⁸ Geometry optimizations were carried out without any symmetry restrictions; the nature of the minima was verified with analytical frequency calculations. All total energies and Gibbs free energies have been zero-point energy (ZPE) and temperature corrected using unscaled density functional frequencies. The electronic structure of the different complexes was studied using natural bond orbital analysis (NBO-5 program).⁵⁹ The electron density of the optimized structures was subjected to an atoms in molecules analysis (QTAIM analysis).⁶⁰

■ ASSOCIATED CONTENT

■ Supporting Information

Text, figures, tables, and CIF files giving characterization of the products of catalysis, details of normal- and high-resolution XRD studies, details of computational studies, Z matrices, and NMR spectra. This material is available free of charge via the Internet at <http://pubs.acs.org>.

■ AUTHOR INFORMATION

Notes

The authors declare no competing financial interest.

■ ACKNOWLEDGMENTS

This work was supported by the CNRS and the ANR (programme blanc ANR-08-BLAN-0137-01). R.B. thanks the French MESR for a Ph.D. fellowship. J.-B.S. and C.D. are grateful to the Université Rennes 1, the CNRS, Rennes Métropole, and the Ministère de l'Enseignement Supérieur et de la Recherche for financial support. T.D. is grateful to the "Région Bretagne" for a grant "CREATE", and L.C.M.C. is grateful to the Ministère des Affaires Étrangères and the Fundacion Gran Mariscal de Ayacucho for a grant.

■ REFERENCES

- (1) For representative recent reviews on iron catalysis, see: (a) Gopalaiah, K. *Chem. Rev.* **2013**, *113*, 3248. (b) Sun, C.-L.; Li, B.-J.; Shi, Z.-J. *Chem. Rev.* **2011**, *111*, 1293. (c) Le Bailly, B. A. F.; Thomas, S. P. *RSC Adv* **2011**, *1*, 1435. (d) Junge, K.; Schröder, K.; Beller, M. *Chem. Commun.* **2011**, *47*, 4849. (e) Nakamura, E.; Yoshikai, N. *J. Org. Chem.* **2010**, *75*, 6061. (f) Czaplik, W. M.; Mayer, M.; Cvengros, J.; von Wangelin, A. *J. ChemSusChem* **2009**, *2*, 396. (g) Morris, R. H. *Chem. Soc. Rev.* **2009**, *38*, 2282. (h) Bauer, E. B. *Curr. Org. Chem.* **2008**, *12*, 1341. (i) Correa, A.; Mancheño, O. G.; Bolm, C. *Chem. Soc. Rev.* **2008**, *37*, 1108. (j) Sherry, B. D.; Fürstner, A. *Acc. Chem. Res.* **2008**, *41*, 1500. (k) Fürstner, A.; Martin, R. *Chem. Lett.* **2005**, *34*, 624. (l) Bolm, C.; Legros, J.; Le Paih, J.; Zani, L. *Chem. Rev.* **2004**, *104*, 6217.
- (2) Selected highlights on iron catalysis: (a) Mancheño, O. G. *Angew. Chem., Int. Ed.* **2011**, *50*, 2216. (b) Fürstner, A. *Angew. Chem., Int. Ed.* **2009**, *48*, 1364. (c) Enthaler, S.; Junge, K.; Beller, M. *Angew. Chem., Int. Ed.* **2008**, *47*, 3317. (d) Bullock, R. *Angew. Chem., Int. Ed.* **2007**, *46*, 7360.
- (3) Selected representative and recent examples of iron complexes stabilized by polydentate ligands: (a) Hoyt, J. M.; Sylvester, K. T.; Semproni, S. P.; Chirik, P. J. *J. Am. Chem. Soc.* **2013**, *135*, 4862. (b) Fleischer, S.; Zhou, S.; Junge, K.; Beller, M. *Angew. Chem., Int. Ed.* **2013**, *52*, 5120. (c) Mikhailine, A. A.; Maishan, M. I.; Lough, A. J.; Morris, R. H. *J. Am. Chem. Soc.* **2012**, *134*, 12266. (d) Ziebart, C.; Federsel, C.; Anbarasan, P.; Jackstell, R.; Baumann, W.; Spannenberg, A.; Beller, M. *J. Am. Chem. Soc.* **2012**, *134*, 20701. (e) Prokopchuk, D. E.; Sonnenberg, J. F.; Meyer, N.; Zimmer-De Iulius, M.; Lough, A. J.; Morris, R. H. *Organometallics* **2012**, *31*, 3056. (f) Langer, R.; Diskin-Posner, Y.; Leitus, G.; Shimon, L. J. W.; Ben-David, Y.; Milstein, D. *Angew. Chem., Int. Ed.* **2011**, *50*, 9948. (g) Langer, R.; Leitus, G.; Ben-David, Y.; Milstein, D. *Angew. Chem., Int. Ed.* **2011**, *50*, 2120. (h) Federsel, C.; Boddien, A.; Jackstell, R.; Jennerjahn, R.; Dyson, P. J.; Scopelliti, R.; Laurenczy, G.; Beller, M. *Angew. Chem., Int. Ed.* **2010**, *49*, 9777.
- (4) For monographs, see: (a) Díez-González, S. *N-Heterocyclic Carbenes*; RSC: Cambridge, U.K., 2011. (b) Cazin, C. S. J. *N-Heterocyclic Carbenes in Transition Metal Catalysis and Organocatalysis*. In *Catalysis by metal complexes*; Springer: Berlin, Germany, 2011; Vol. 32. (c) Glorius, F. *N-Heterocyclic Carbenes in Transition Metal Catalysis*. In *Topics in Organometallic Chemistry*; Springer: Berlin, Germany, 2007; Vol. 21. (d) Nolan, S. P. *N-Heterocyclic Carbenes in Synthesis*; Wiley-VCH: Weinheim, Germany, 2007.

- (5) For selected reviews, see: (a) Valente, C.; Çalimsiz, S.; Hoi, K. H.; Mallik, D.; Sayah, M.; Organ, M. G. *Angew. Chem., Int. Ed.* **2012**, *51*, 3314. (b) Benhamou, L.; Chardon, E.; Lavigne, G.; Bellemin-Lapponnaz, S.; César, V. *Chem. Rev.* **2011**, *111*, 2705. (c) Melaimi, M.; Soleilhavoup, M.; Bertrand, G. *Angew. Chem., Int. Ed.* **2010**, *49*, 8810. (d) Dröge, T.; Glorius, F. *Angew. Chem., Int. Ed.* **2010**, *49*, 6940. (e) Clavier, H.; Nolan, S. P. *Chem. Commun.* **2010**, *46*, 841. (f) Merces, L.; Albrecht, M. *Chem. Soc. Rev.* **2010**, *39*, 1903. (g) Díez-González, S.; Marion, N.; Nolan, S. P. *Chem. Rev.* **2009**, *109*, 3612. (h) Samojłowicz, C.; Bieniek, M.; Grela, K. *Chem. Rev.* **2009**, *109*, 3708. (i) Poyatos, M.; Mata, J. A.; Peris, E. *Chem. Rev.* **2009**, *109*, 3677. (j) Lin, J. C. Y.; Huang, R. T. W.; Lee, C. S.; Bhattacharyya, A.; Hwang, W. S.; Lin, I. J. B. *Chem. Rev.* **2009**, *109*, 3561. (k) Jacobsen, H.; Correa, A.; Poater, A.; Costabile, C.; Cavallo, L. *Coord. Chem. Rev.* **2009**, *253*, 687. (l) Hahn, F. E.; Jahnke, M. C. *Angew. Chem., Int. Ed.* **2008**, *47*, 3122. (m) Díez-González, S.; Nolan, S. P. *Acc. Chem. Res.* **2008**, *41*, 349. (n) Cavell, K. *Dalton Trans.* **2008**, 6676. (o) César, V.; Bellemin-Lapponnaz, S.; Gade, L. H. *Chem. Soc. Rev.* **2004**, *33*, 619. (p) Bourissou, D.; Guerret, O.; Gabbai, F. P.; Bertrand, G. *Chem. Rev.* **2000**, *100*, 39.
- (6) Reviews on Fe-NHC complexes: (a) Bézier, D.; Sortais, J.-B.; Darcel, C. *Adv. Synth. Catal.* **2013**, *355*, 19. (b) Ingleson, M. J.; Layfield, R. A. *Chem. Commun.* **2012**, *48*, 3579.
- (7) (a) Grohmann, C.; Hashimoto, T.; Fröhlich, R.; Ohki, Y.; Tatsumi, K.; Glorius, F. *Organometallics* **2012**, *31*, 8047. (b) Kaplan, H. Z.; Li, B.; Byers, J. A. *Organometallics* **2012**, *31*, 7343. (c) Merces, L.; Labat, G.; Neels, A.; Ehlers, A.; Albrecht, M. *Organometallics* **2006**, *25*, 5648 and references therein.
- (8) Well-defined monodentate NHC-containing Fe complexes: (a) Danopoulos, A. A.; Monakhov, K. Y.; Braunstein, P. *Chem. Eur. J.* **2013**, *19*, 450. (b) Zhang, Q.; Xiang, L.; Deng, L. *Organometallics* **2012**, *31*, 4537. (c) Wang, X.; Mo, Z.; Xiao, J.; Deng, L. *Inorg. Chem.* **2012**, *52*, 59. (d) Przyojski, J. A.; Arman, H. D.; Tonzetich, Z. J. *Organometallics* **2012**, *31*, 3264. (e) Danopoulos, A. A.; Braunstein, P.; Wesolek, M.; Monakhov, K. Y.; Rabu, P.; Robert, V. *Organometallics* **2012**, *31*, 4102. (f) Danopoulos, A. A.; Braunstein, P.; Stylianides, N.; Wesolek, M. *Organometallics* **2011**, *30*, 6514. (g) Hatanaka, T.; Ohki, Y.; Tatsumi, K. *Chem. Asian J.* **2010**, *5*, 1657. (h) Holzwarth, M.; Dieskau, A.; Tabassam, M.; Plietker, B. *Angew. Chem., Int. Ed.* **2009**, *48*, 7251. (i) Ohki, Y.; Hatanaka, T.; Tatsumi, K. *J. Am. Chem. Soc.* **2008**, *130*, 17174. (j) Louie, J.; Grubbs, R. H. *Chem. Commun.* **2000**, 1479.
- (9) (a) Brunner, H.; Rötzer, J. *Organomet. Chem.* **1992**, *425*, 119. (b) Fisch, K.; Brunner, H. *J. Organomet. Chem.* **1991**, *412*, C11. (c) Brunner, H. *Angew. Chem., Int. Ed. Engl.* **1990**, *29*, 1131.
- (10) (a) Cardoso, J. M. S.; Royo, B. *Chem. Commun.* **2012**, *48*, 4944. (b) Kandepi, V. V. K. M.; Cardoso, J. M. S.; Peris, E.; Royo, B. *Organometallics* **2010**, *29*, 2777.
- (11) For a review on the Fe-catalyzed reduction of carbonyl functionalities see: Chakraborty, S.; Guan, H. *Dalton Trans.* **2010**, *39*, 7427.
- (12) (a) Misal Castro, L. C.; Sortais, J.-B.; Darcel, C. *Chem. Commun.* **2012**, *48*, 151. (b) Bézier, D.; Jiang, F.; Sortais, J.-B.; Darcel, C. *Eur. J. Inorg. Chem.* **2012**, 1333. (c) Bézier, D.; Venkanna, G. T.; Sortais, J.-B.; Darcel, C. *ChemCatChem* **2011**, *3*, 1747. (d) Jiang, F.; Bézier, D.; Sortais, J.-B.; Darcel, C. *Adv. Synth. Catal.* **2011**, *353*, 239.
- (13) Buchgraber, P.; Toupet, L.; Guerschais, V. *Organometallics* **2003**, *22*, 5144.
- (14) Hashimoto, T.; Urban, S.; Hoshino, R.; Ohki, Y.; Tatsumi, K.; Glorius, F. *Organometallics* **2012**, *31*, 4474.
- (15) (a) Warratz, S.; Postigo, L.; Royo, B. *Organometallics* **2013**, *32*, 893. (b) Li, H.; Misal Castro, L. C.; Zheng, J.; Roisnel, T.; Dorcet, V.; Sortais, J. B.; Darcel, C. *Angew. Chem., Int. Ed.* **2013**, *52*, 8045.
- (16) Photoswitchable NHCs: (a) Neilson, B. M.; Bielawski, C. W. *J. Am. Chem. Soc.* **2012**, *134*, 12693. (b) Neilson, B. M.; Lynch, V. M.; Bielawski, C. W. *Angew. Chem., Int. Ed.* **2011**, *50*, 10322. Redox-switchable NHCs: (c) Tennyson, A. G.; Lynch, V. M.; Bielawski, C. W. *J. Am. Chem. Soc.* **2010**, *132*, 9420. (d) Rosen, E. L.; Varnado, C. D.; Tennyson, A. G.; Khramov, D. M.; Kamplain, J. W.; Sung, D. H.; Cresswell, P. T.; Lynch, V. M.; Bielawski, C. W. *Organometallics* **2009**, *28*, 6695. (e) Siemeling, U.; Färber, C.; Leibold, M.; Bruhn, C.; Mücke, P.; Winter, R. F.; Sarkar, B.; Von Hopffgarten, M.; Frenking, G. *Eur. J. Inorg. Chem.* **2009**, 4607. (f) Khramov, D. M.; Rosen, E. L.; Lynch, V. M.; Bielawski, C. W. *Angew. Chem., Int. Ed.* **2008**, *47*, 2267. Acid-base switchable NHCs: (g) Reference 19. (h) Hashmi, A. S. K.; Lothschütz, C.; Graf, K.; Häffner, T.; Schuster, A.; Rominger, F. *Adv. Synth. Catal.* **2011**, *353*, 1407. (i) Biju, A.; Hirano, K.; Fröhlich, R.; Glorius, F. *Chem. Asian J.* **2009**, *4*, 1786. Tunable NHCs: (j) Alcarazo, M.; Stork, T.; Anoop, A.; Thiel, W.; Fürstner, A. *Angew. Chem., Int. Ed.* **2010**, *49*, 2542. (k) Ogle, J. W.; Miller, S. A. *Chem. Commun.* **2009**, 5728. (l) Leuthäuser, S.; Schmidts, V.; Thiele, C. M.; Plenio, H. *Chem. Eur. J.* **2008**, *14*, 5465. (m) Präsang, C.; Donnadiu, B.; Bertrand, G. *J. Am. Chem. Soc.* **2005**, *127*, 10182.
- (17) Malonyl-derived NHCs: (a) César, V.; Barthes, C.; Farré, Y. C.; Cuisiat, S. V.; Vacher, B. Y.; Brousses, R.; Lugan, N.; Lavigne, G. *Dalton Trans.* **2013**, *42*, 7373. (b) César, V.; Lugan, N.; Lavigne, G. *Chem. Eur. J.* **2010**, *16*, 11432. (c) César, V.; Lugan, N.; Lavigne, G. *Eur. J. Inorg. Chem.* **2010**, 361. (d) César, V.; Lugan, N.; Lavigne, G. *J. Am. Chem. Soc.* **2008**, *130*, 11286.
- (18) Imidate-derived NHC: Vujkovic, N.; César, V.; Lugan, N.; Lavigne, G. *Chem. Eur. J.* **2011**, *17*, 13151.
- (19) Five-membered NHCs: (a) César, V.; Tourneux, J. C.; Vujkovic, N.; Brousses, R.; Lugan, N.; Lavigne, G. *Chem. Commun.* **2012**, *48*, 2349. (b) Benhamou, L.; Vujkovic, N.; César, V.; Gornitzka, H.; Lugan, N.; Lavigne, G. *Organometallics* **2010**, *29*, 2616. (c) Benhamou, L.; César, V.; Gornitzka, H.; Lugan, N.; Lavigne, G. *Chem. Commun.* **2009**, 4720.
- (20) Note: in the nomenclature adopted in this work, the label numbers for all complexes and NHC ligands are associated with a subscript corresponding to the nature of the central R substituent of the malonate backbone and, where applicable, a superscript indicating that the backbone has been alkylated.
- (21) (a) Wolf, S.; Plenio, H. *J. Organomet. Chem.* **2009**, *694*, 1487. (b) Kelly, R. A. I.; Clavier, H.; Giudice, S.; Scott, N. M.; Stevens, E. D.; Bordner, J.; Samardjiev, I.; Hoff, C. D.; Cavallo, L.; Nolan, S. P. *Organometallics* **2007**, *27*, 202.
- (22) Mushinski, R. M.; Squires, B. M.; Sincerbox, K. A.; Hudnall, T. W. *Organometallics* **2012**, *31*, 4862.
- (23) Six-membered diamidocarbenes: (a) Moerdyk, J. P.; Bielawski, C. W. *Nat. Chem.* **2012**, *4*, 275. (b) Moerdyk, J. P.; Bielawski, C. W. *J. Am. Chem. Soc.* **2012**, *134*, 6116. (c) Moerdyk, J. P.; Bielawski, C. W. *Organometallics* **2011**, *30*, 2278. (d) Hudnall, T. W.; Moorhead, E. J.; Gusev, D. G.; Bielawski, C. W. *J. Org. Chem.* **2010**, *75*, 2763. (e) Hudnall, T. W.; Moerdyk, J. P.; Bielawski, C. W. *Chem. Commun.* **2010**, *46*, 4288. (f) Hudnall, T. W.; Bielawski, C. W. *J. Am. Chem. Soc.* **2009**, *131*, 16039. Five-membered diamidocarbenes: (g) Braun, M.; Frank, W.; Ganter, C. *Organometallics* **2012**, *31*, 1927. (h) Braun, M.; Frank, W.; Reiss, G. J.; Ganter, C. *Organometallics* **2010**, *29*, 4418. Seven-membered diamidocarbene: (i) Hudnall, T. W.; Tennyson, A. G.; Bielawski, C. W. *Organometallics* **2010**, *29*, 4569.
- (24) For a review on the ¹³C NMR characterization of carbenes, see: Tapu, D.; Dixon, D. A.; Roe, C. *Chem. Rev.* **2009**, *109*, 3385.
- (25) Allen, F. H.; Kennard, O.; Watson, D. G.; Brammer, L.; Orpen, A. G.; Taylor, R. *J. Chem. Soc., Perkin Trans. 2* **1987**, S1.
- (26) Pauling, L. *The Nature of the Chemical Bond*; Cornell University Press: Ithaca, NY, 1960; p 144. Parameters taken from reference 27.
- (27) Howard, S. T.; Lamarche, O. *J. Phys. Org. Chem.* **2003**, *16*, 133.
- (28) For reviews explaining the metal-NHC bond, see: (a) Jacobsen, H.; Correa, A.; Poater, A.; Costabile, C.; Cavallo, L. *Coord. Chem. Rev.* **2009**, *253*, 687. (b) Radius, U.; Bickelhaupt, F. M. *Coord. Chem. Rev.* **2009**, *253*, 678. For reports showing the non-negligible π -back-donating interaction between metal and NHC, see: (c) Fantasia, S.; Petersen, J. L.; Jacobsen, H.; Cavallo, L.; Nolan, S. P. *Organometallics* **2007**, *26*, 5880. (d) Sanderson, M. D.; Kamplain, J. W.; Bielawski, C. W. *J. Am. Chem. Soc.* **2006**, *128*, 16514. (e) Hu, X.; Castro-Rodriguez, I.; Olsen, K.; Meyer, K. *Organometallics* **2004**, *23*, 755.
- (29) (a) Fernández, I.; Lugan, N.; Lavigne, G. *Organometallics* **2012**, *31*, 1155. (b) Valyaev, D. A.; Brousses, R.; Lugan, N.; Fernández, I.; Sierra, M. A. *Chem. Eur. J.* **2011**, *17*, 6602.

- (30) Credendino, R.; Falivene, L.; Cavallo, L. *J. Am. Chem. Soc.* **2012**, *134*, 8127.
- (31) For an earlier experimental charge density analysis of an N-methyl-substituted NHC [Cr(0)] carbene complex see: Tafipolsky, M.; Scherer, W.; Öfele, K.; Artus, G.; Pedersen, B.; Herrmann, W. A.; McGrady, G. S. *J. Am. Chem. Soc.* **2002**, *124*, 5865.
- (32) Hansen, N. K.; Coppens, P. *Acta Crystallogr.* **1978**, *A34*, 909.
- (33) (a) Frisch, M. J.; Trucks, G. W.; Schlegel, H. B.; Scuseria, G. E.; Robb, M. A.; Cheeseman, J. R.; Scalmani, G.; Barone, V.; Mennucci, B.; Petersson, G. A.; Nakatsuji, H.; Caricato, M.; Li, X.; Hratchian, H. P.; Izmaylov, A. F.; Bloino, J.; Zheng, G.; Sonnenberg, J. L.; Hada, M.; Ehara, M.; Toyota, K.; Fukuda, R.; Hasegawa, J.; Ishida, M.; Nakajima, T.; Honda, Y.; Kitao, O.; Nakai, H.; Vreven, T.; Montgomery, J. A., Jr.; Peralta, J. E.; Ogliaro, F.; Bearpark, M.; Heyd, J. J.; Brothers, E.; Kudin, K. N.; Staroverov, V. N.; Kobayashi, R.; Normand, J.; Raghavachari, K.; Rendell, A.; Burant, J. C.; Iyengar, S. S.; Tomasi, J.; Cossi, M.; Rega, N.; Millam, J. M.; Klene, M.; Knox, J. E.; Cross, J. B.; Bakken, V.; Adamo, C.; Jaramillo, J.; Gomperts, R.; Stratmann, R. E.; Yazyev, O.; Austin, A. J.; Cammi, R.; Pomelli, C.; Ochterski, J. W.; Martin, R. L.; Morokuma, K.; Zakrzewski, V. G.; Voth, G. A.; Salvador, P.; Dannenberg, J. J.; Dapprich, S.; Daniels, A. D.; Farkas, Ö.; Foresman, J. B.; Ortiz, J. V.; Cioslowski, J.; Fox, D. J. *Gaussian 09, Revision C.01*; Gaussian, Inc., Wallingford, CT, 2009. (b) See the Supporting Information for computational details.
- (34) (a) Farrugia, L.; Evans, C. *J. Phys. Chem. A* **2005**, *109*, 8834. (b) Farrugia, L.; Mallinson, P. R.; Stewart, B. *Acta Crystallogr., Sect. B* **2003**, *59*, 234 and references therein.
- (35) The complete tables, along with residual and Laplacian maps in selected planes, are provided in the Supporting Information.
- (36) The ideal [5, S, 1 + 1] topology for a Cp ring associated to a metal has actually rarely been observed, the MC bcp's and the MC₂ rcp's within the MCp unit often merging due to their intrinsic proximity in a topological catastrophe scheme. For a detailed study, see: (a) Farrugia, L.; Evans, C.; Lentz, D.; Roemert, M. *J. Am. Chem. Soc.* **2009**, *131*, 1251 and references therein. (b) Borissova, A. O.; Antipin, M. Y.; Lyssenko, K. A. *J. Phys. Chem. A* **2009**, *113*, 10845.
- (37) Macchi, P.; Sironi, A. *Coord. Chem. Rev.* **2003**, *238*, 383.
- (38) (a) Farrugia, L. J.; Evans, C.; Senn, H. M.; Hänninen, M. M.; Sillanpää, R. *Organometallics* **2012**, *31*, 2559. (b) Farrugia, L. J.; Senn, H. M. *J. Phys. Chem. A* **2010**, *114*, 13418. (c) Farrugia, L.; Evans, C.; Lentz, D.; Roemert, M. *J. Am. Chem. Soc.* **2009**, *131*, 1251. (d) Farrugia, L.; Evans, C.; Tegel, M. *J. Phys. Chem. A* **2006**, *110*, 7952. (e) Farrugia, L.; Evans, C. *J. Phys. Chem. A* **2005**, *109*, 8834.
- (39) Koch, U.; Popelier, P. L. A. *J. Phys. Chem.* **1995**, *99*, 9747.
- (40) (a) Espinosa, E.; Alkorta, I.; Rozas, I.; Elguero, J.; Molins, E. *Chem. Phys. Lett.* **2001**, *336*, 457. (b) Espinosa, E.; Molins, E.; Lecomte, C. *Chem. Phys. Lett.* **1998**, *285*, 170.
- (41) (a) $E_{\text{int}} = -313.754[V(r_b)]$, where E_{int} is the interaction energy (in kcal mol⁻¹) and $V(r_b)$ is the potential energy density (in au). (b) Nelyubina, Y. V.; Antipin, M. Y.; Lyssenko, K. A. *Russ. Chem. Rev.* **2010**, *79*, 167.
- (42) Abramov, Y. A. *Acta Crystallogr., Sect. A* **1997**, *53*, 264.
- (43) (a) Fradera, X.; Austen, M. A.; Bader, R. F. W. *J. Phys. Chem. A* **1999**, *103*, 304. (b) Bader, R. F. W.; Stephens, M. E. *J. Am. Chem. Soc.* **1975**, *97*, 7391.
- (44) The reaction yield is strongly reduced by using 0.5 mol % of complex **11**.
- (45) Data taken from: Fulmer, G. R.; Miller, A. J. M.; Sherden, N. H.; Gottlieb, H. E.; Nudelman, A.; Stoltz, B. M.; Bercaw, J. E.; Goldberg, K. I. *Organometallics* **2010**, *29*, 2176.
- (46) Yasuda, S.; Yorimitsu, H.; Ashima, K. *Organometallics* **2008**, *27*, 4025.
- (47) APEX2 (Version 2011.2-0); Bruker AXS Inc., Madison, WI.
- (48) Farrugia, L. J. *J. Appl. Crystallogr.* **1999**, *32*, 837.
- (49) Altomare, A.; Cascarano, G.; Giacovazzo, C.; Guagliardi, A. *J. Appl. Crystallogr.* **1993**, *26*, 343.
- (50) Sheldrick, G. M. *Acta Crystallogr.* **2008**, *A64*, 112.
- (51) Blessing, R. H. *J. Appl. Crystallogr.* **1989**, *22*, 396.
- (52) Jelsch, C.; Guillot, B.; Lagoutte, A.; Lecomte, C. *J. Appl. Crystallogr.* **2004**, *38*, 38.
- (53) Madsen, O. *J. Appl. Crystallogr.* **2006**, *39*, 757.
- (54) SHADE2 server: <http://shade.ki.ku.dk/docs/index.html>.
- (55) Hirsfeld, F. L. *Acta Crystallogr.* **1976**, *A32*, 239.
- (56) Stash, A.; Tsirelson, V. *J. Appl. Crystallogr.* **2002**, *35*, 371.
- (57) Zhao, Y.; Truhlar, D. G. *Theor. Chem. Acc.* **2008**, *120*, 215.
- (58) Hariharan, P. C.; Pople, J. A. *Theor. Chim. Acta* **1973**, *28*, 213.
- (59) (a) Glendening, E. D.; Badenhop, J. K.; Reed, A. E.; Carpenter, J. E.; Bohmann, J. A.; Morales, C. M.; Weinhold, F. *NBO 5.0*; Theoretical Chemistry Institute, University of Wisconsin, Madison, WI, 2001. (b) Reed, E.; Curtiss, L. A.; Weinhold, F. *Chem. Rev.* **1988**, *88*, 899. (c) Reed, A. E.; Weinhold, F. *J. Chem. Phys.* **1985**, *83*, 1736. (d) Foster, J. P.; Weinhold, F. *J. Am. Chem. Soc.* **1980**, *102*, 7211.
- (60) (a) Bader, R. F. W. *Atoms in Molecules: A Quantum Theory*; Oxford University Press: New York, 1990. (b) Bader, R. F. W. *Chem. Rev.* **1991**, *91*, 893. (c) Keith, T. A. *AIMAll (Version 10.10.11)*, 2010 (aim.tkgristmill.com).